31

Vertical Jump: Biomechanical Analysis and Simulation Study

Jan Babič and Jadran Lenarčič
"Jožef Stefan" Institute
Slovenia

1. Introduction

Vertical jumping is a complex task requiring quick and harmonized coordination of jumper's body segments, first for the push-off, then for the flight and lastly for the landing. The prime criterion for vertical jump efficiency is the height of the jump that depends on the speed of the jumper's center of gravity (COG) in the moment when the feet detach from the ground. Besides maintaining the balance, the task of the muscles during the push-off phase of the jump is to accelerate the body's COG up in the vertical direction to the extended body position. During the push-off phase of the jump, the jumper's center of gravity must be above the supporting polygon that is formed by the feet (Babič et al., 2001). In contrast to the humans, today's humanoid robots are mostly unable to perform fast movements such as the vertical jump. They can mostly perform only slow and statically stable movements that do not imitate the human motion. Besides, these slow and statically stable movements are energy inefficient. With the understanding of the anatomy and the biomechanics of the human body, one can find out that, beside the shape, majority of today's humanoid robots and human bodies do not have a lot of common properties. To achieve a better imitation of the human motion and ability to perform fast movements such as the vertical jump or running, other properties and particularities, beside the shape of the body, should be considered in the design of the humanoid robot.

Lower extremities of today's humanoid robots are mostly serial mechanisms with simple rotational joints that are driven directly or indirectly by electrical servo drives. Such design of humanoid robot mechanism allows only rotational motion in joints to occur. This means that translations of the robot's center of gravity are solely a result of the transformation of rotations in joints into translations of the robot center of gravity. Especially in ballistic movements such as fast running or jumping where the robot center of gravity is to be accelerated from low or zero velocity to a velocity as high as possible, this transformation is handicapped. The transfer of the angular motion of the lower extremity segments to the desired translational motion of the robot center of gravity is less effective the more the joints are extended. When the joint is fully extended, the effect of this joint on the translational motion of the robot center of gravity in a certain direction equals zero. Besides, the motion of the segments should decelerate to zero prior to the full extension to prevent a possible damaging hyperextension. Where relatively large segments which may contain considerable amounts of rotational energy are involved, high power is necessary to decelerate the angular motion.

Source: Humanoid Robots, New Developments, Book edited by: Armando Carlos de Pina Filho
ISBN 978-3-902613-02-8, pp.582, I-Tech, Vienna, Austria, June 2007

Servo drives that drive the joints of the humanoid robot represent a model of the group of monoarticular muscles that are passing a single joint and thus cause a rotational motion of the joint that are passing. Beside the monoarticular muscles that are passing only one joint, human lower extremity consists of another group of muscles that are passing two joints. These muscles are so called biarticular muscles. Their functions during human movement have been studied extensively by many researchers. One of such functions is the transportation of mechanical energy from proximal to distal joints. It is believed that this transportation causes an effective transformation of rotational motion of body segments into translation of the body centre of gravity (Schenau, 1989). Gastrocnemius muscle is a biarticular muscle that is passing the knee and the ankle joints and acts as a knee flexor and ankle extensor (see Fig. 1).

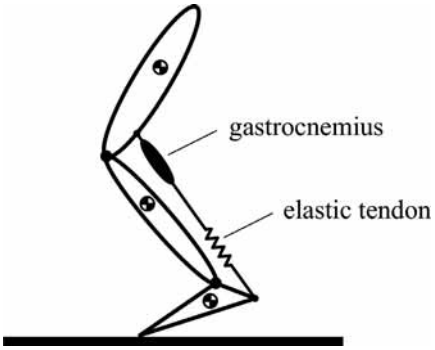

Fig. 1. Biarticular muscle gastrocnemius passing the knee and the ankle joints. It acts as a knee flexor and ankle extensor. Gastrocnemius muscle is connected to the foot by an elastic tendon.

In jumping, the activation of the biarticular gastrocnemius muscle prior to the end of the push-off enables the transportation of the power generated by the knee extensors from the knee to the ankle joint. This transfer of mechanical energy by gastrocnemius can be explained using the following example. During the push-off phase of the jump, the knee joint is rapidly extended as a result of the positive work done by the knee extensor muscles. If the biarticular gastrocnemius muscle contracts isometrically (its length does not change), the additional mechanical work is done at the ankle joint because of the gastrocnemius muscle, which contributes no mechanical work by itself. A part of the energy generated by the knee extensors appears as mechanical work at the ankle joint and the height of the jump is significantly increased. This is because, as the jump proceeds and the knee straightens, the angular position changes of the knee have progressively less effect on vertical velocity of the jumper's centre of gravity. By gastrocnemius muscle activation, a rapid extension of the foot is produced. This extension has a greater effect on the vertical velocity than the extension of the almost straightened knee. The energy is more effectively translated into vertical velocity and a greater height of the jump is achieved. However, the timing of the gastrocnemius muscle activation is critical to obtain a maximum effect. This was demonstrated by an articulated physical model of the vertical jump by Bobbert et al (1986).

Besides biarticularity, the gastrocnemius muscle has one more interesting feature. It is connected to the foot by an elastic tendon (see Fig. 1). The elasticity in the muscle fibers and tendons plays an important role in enhancing the effectiveness and the efficiency of human performance. An enhanced performance of human motion has been most effectively

demonstrated for jumping and running (Cavagna, 1970; Bobbert et al., 1996; Shorten, 1985). An important feature of elastic tissues is the ability to store elastic energy when stretched and to recoil this energy afterwards as a mechanical work (Asmussen and Bonde-Petersen, 1974). Beside this feature, oscillatory movements performed at the natural frequency of muscle-tendon complex could maximize the performance. A countermovement vertical jump can be treated as one period of oscillatory movement and from this point of view the natural frequency, as well as parameters that define the natural frequency, can be determined.

The purpose of our research was twofold. First to analyse the human vertical jump and to show that for each and every subject there exists an optimal triceps surae muscle-tendon complex stiffness that ensures the maximal possible height of the vertical jump. We defined the influence of the m. gastrocnemius activation timing and the m. gastrocnemius and Achilles tendon stiffness on the height of the vertical jump and established the methodology for analysis and evaluation of the vertical jump. We monitored kinematics, dynamics and m. gastrocnemius electrical activity during the maximum height countermovement jump of human subjects and measured viscoelastic properties of the m. gastrocnemius and Achilles tendon using the free-vibration technique. Based on the findings of the biomechanical study of the human vertical jump we performed a simulation study of the humanoid robot vertical jump. As a result of our research we propose a new human inspired structure of the lower extremity mechanism by which a humanoid robot would be able to efficiently perform fast movements such as running and jumping.

2. Biorobotic Model of Vertical Jump

Biorobotic model of the vertical jump consists of the dynamic model of the musculoskeletal system and of the mathematical model used for the motion control of the model. The results of the modelling are differential equations and a diagram for simulation and optimization of the vertical jump.

2.1 Dynamic Model of Musculoskeletal System

Vertical jump is an example of a movement that can be satisfactorily observed and analyzed in just a sagital plane. Therefore we built a model of the musculoskeletal system in a two dimensional space of the sagital plane. Because both lower extremities perform the same movement during the vertical jump, we joined both extremities in one extremity with three rigid body segments. Trunk, head and upper extremities were modeled as one rigid body with a common COG, mass and moment of inertia. The model of the musculoskeletal system is therefore a planar model composed of four segments that represent the foot, shank, thigh and trunk together with the head and both upper extremities. Segments of the model are joined together by frictionless rotational hinges whose axes are perpendicular to the sagital plane. The contact between the foot and the ground is modeled as a rotational joint between the tip of the foot and the ground. A model, whose foot is connected to the ground by a rotational joint, is applicable only for the push-off and landing phases of the vertical jump and is not applicable for the flight. As the motion of the COG during the flight is simply described and depends only on the speed vector of the COG just prior to the takeoff, this simplification does not present any limitations.

Fig. 2 shows the planar model of the musculoskeletal system, composed of four rigid bodies that represent the foot, shank, thigh and trunk together with the head and both upper extremities. The origin of the base coordinate system is in the center of the virtual joint that connects the foot with the ground.

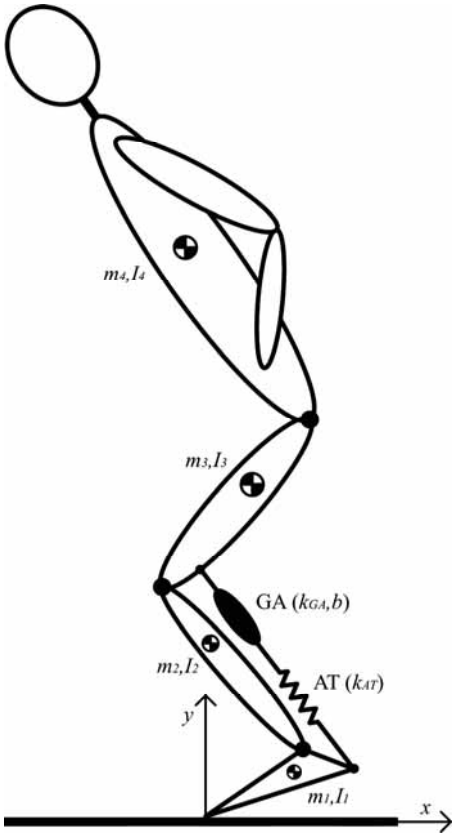

Fig. 2. Planar model of the musculoskeletal system

Passive constraints in the hip, knee and ankle that define the range of motion of these joints were modeled as simple nonlinear springs (Audu and Davy, 1985; Davy and Audu, 1987).
Fig. 2 also shows the model of the biarticular link that consists of the gastrocnemius muscle (GA) with stiffness k_{GA} and damping b and the Achilles tendon (AT) with stiffness k_{AT}. Contrary to the real gastrocnemius muscle, biarticular link can not contract. It can only be enabled or disabled at different moments during the push-off phase of the jump. High pennation angle of the gastrocnemius muscle fibers suggest that the predominant role of the m. gastrocnemius is not in its contraction but in its ability to bear high forces and to enable the energy transportation from the knee to the ankle (Bogert et al., 1989; Legreneur et al., 1997). Therefore our simulated biarticular link that can not contract and can only be enabled or disabled is considered as an appropriate model for this study.
Insertions of the biarticular link on the foot (B) and thigh (C) have been determined from the muscle data provided by Brand et al. (1982) and Delp (1990).

Vector of the force in the biarticular link $\boldsymbol{f}$ is

$$f = k \cdot (BC - BC_0) - b \cdot BC \,, \tag{1}$$

where k represents the stiffness of the m. gastrocnemius and Achilles tendon connected in series, $\boldsymbol{BC}$ is the vector between the insertions of the biarticular link on the foot and thigh. $\boldsymbol{BC}_0$ is the vector $\boldsymbol{BC}$ in the moment of the gastrocnemius muscle activation. Force in the biarticular link $\boldsymbol{f}$ causes a torque in the ankle joint

$$Q_{bl2} = -\left\| \boldsymbol{r}_B \times \boldsymbol{f} \right\| , \tag{2}$$

where $\boldsymbol{r}_B$ is the moment arm vector from the center of the ankle joint to the insertion of the biarticular link on the foot and a torque in the knee joint

$$Q_{bl3} = \left\| \boldsymbol{r}_C \times \boldsymbol{f} \right\| , \tag{3}$$

where $\boldsymbol{r}_C$ is the moment arm vector from the center of the knee joint to the insertion of the biarticular link on the thigh.

Motion of the musculoskeletal system is written with a system of dynamic equations of motion

$$\mathbf{H}(\boldsymbol{q})\ddot{\boldsymbol{q}} + \boldsymbol{h}(\boldsymbol{q}, \dot{\boldsymbol{q}}) + \boldsymbol{G}(\boldsymbol{q}) = \boldsymbol{Q}_{mov} + \boldsymbol{Q}_{pas} + \boldsymbol{Q}_{bl} \,, \tag{4}$$

where $\boldsymbol{Q}_{pas}$ is the vector of joint torques caused by the passive constraints and $\boldsymbol{Q}_{bl}$ is the vector of joint torques caused by the biarticular link. $\boldsymbol{Q}_{mov}$ is the vector of joint torques caused by muscles and represents the input to the direct dynamic model of the musculoskeletal system. The output from the direct dynamic model is the vector of joint displacements $\boldsymbol{q}$. We determined parameters of (4) $\mathbf{H}(\boldsymbol{q}), \boldsymbol{h}(\boldsymbol{q}, \dot{\boldsymbol{q}}), \boldsymbol{G}(\boldsymbol{q})$ using the equations published by Asada and Slotine (1986). Simulation diagram of the direct dynamic model of the musculoskeletal system is shown in the shaded rectangle of the Fig. 3.

2.2 Motion Control

Motion controller of the musculoskeletal system was designed to meet the following four requirements:

1. Perpendicular projection of the body's COG on the ground coincides with the virtual joint that connects the foot with the ground during the entire push-off phase of the vertical jump. Therefore balance of the jumper and verticality of the jump is assured. Equation that describes this requirement is

$$x_T^d(t) = 0 \,, \tag{5}$$

where $x_T^d(t)$ is the distance between the desired perpendicular projection of the body's COG on the ground from the origin of the base coordinate system in time t.

2. Motion controller assures the desired vertical movement of the body's COG relative to the ankle $y_{TA}^d(t)$. By controlling the movement of the body's COG relative to the ankle, we excluded the influence of the biarticular link on the motion $y_{TA}^d(t)$. Therefore parameters of the biarticular link can be varied and optimized for a certain desired motion of the body's COG relative to the ankle.

3. Motion controller assures a constant angle of the foot relative to the ground q_1 before the biarticular link activation occurs. Thus the number of degrees of freedom of the model remains constant during the push-off phase of the vertical jump

4. In the moment, when the biarticular link activates, motion controller sets the torque in the ankle joint Q_2 to zero and thus enable a free motion of the foot relative to the ground. By setting the torque in the ankle joint to zero, the motion in the ankle joint is only a function of the motion in the knee joint that is transmitted to the ankle by the biarticular link.

Motion controller that considers the requirement (5) and enables the desired vertical motion of the COG relative to the ankle $y_{TA}^{d}(t)$ in the base coordinate system is

$$\ddot{\boldsymbol{x}}_T^c = \begin{bmatrix} 0 \\ \ddot{y}_{TA}^d + \ddot{y}_A \end{bmatrix} + k_p \left(\begin{bmatrix} 0 \\ y_{TA}^d + y_A \end{bmatrix} - \boldsymbol{x}_T \right) + k_d \left(\begin{bmatrix} 0 \\ \dot{y}_{TA}^d + \dot{y}_A \end{bmatrix} - \dot{\boldsymbol{x}}_T \right), \tag{6}$$

where k_p and k_d are coefficients of the PD controller, $\ddot{\boldsymbol{x}}_T^c$ is the vector of the control acceleration of the COG in the base coordinate system, y_A is the current height of the ankle joint relative to the ground, $\dot{\boldsymbol{x}}_T, \boldsymbol{x}_T$ are the vectors of the current speed and position of the COG in the base coordinate system.

The relation between the vector of the control speed of the COG in the base coordinate system $\dot{\boldsymbol{x}}_T^c$ and the vector of the control angular velocities in the joints $\dot{\boldsymbol{q}}_c$ is

$$\dot{\boldsymbol{x}}_T^c = \mathbf{J}_T \dot{\boldsymbol{q}}_c \,, \tag{7}$$

where $\mathbf{J}_T$ is the Jacobian matrix of the COG speed in the base coordinate system. Equation (7) represents an under determined system of equations. From the requirement that the motion controller assures a constant angle of the foot relative to the ground q_1 before the biarticular link activation occurs, follows the condition

$$\dot{q}_{c1} = 0 \,. \tag{8}$$

An additional condition that abolishes the under determination of (7) is the relationship of the knee and hip joint angles

$$\dot{q}_{c4} = n \cdot \dot{q}_{c3} \,, \tag{9}$$

where n is the coefficient that describes the relationship.

By substitution of (8) and (9) into (7) we get a relation between the vector of the control speed of the COG in the base coordinate system $\dot{\boldsymbol{x}}_T^c$ and the vector of the control angular velocities in the ankle and knee joints $\dot{\boldsymbol{q}}_c'$

$$\dot{\boldsymbol{x}}_T^c = \mathbf{J}_\mathbf{T}' \dot{\boldsymbol{q}}_c' \,, \tag{10}$$

where $\mathbf{J}_\mathbf{T}'$ is a new Jacobian matrix of the center of gravity speed in the base coordinate system. Differentiation of (10) with respect to time yields

$$\ddot{\boldsymbol{q}}_c' = \begin{bmatrix} \ddot{q}_{c2} \\ \ddot{q}_{c3} \end{bmatrix} = \mathbf{J}_T'^{-1} (\ddot{\boldsymbol{x}}_T^c - \dot{\mathbf{J}}_T' \dot{\boldsymbol{q}}') \,, \tag{11}$$

where

$$\dot{\boldsymbol{q}}' = \begin{bmatrix} \dot{q}_2 \\ \dot{q}_3 \end{bmatrix}. \tag{12}$$

On the basis of conditions (8) and (9) and relation (11) we define control angular accelerations in all four joints

$$\ddot{\boldsymbol{q}}_c = \begin{bmatrix} 0 \\ \ddot{q}_{c2} \\ \ddot{q}_{c3} \\ n\ddot{q}_{c3} \end{bmatrix}. \tag{13}$$

By substitution of (13) into a system of dynamic equations of motion (4) we get control torques in joints $\boldsymbol{Q}_{mov}$ that we need to control the model of the musculoskeletal system

$$\boldsymbol{Q}_{mov} = \mathbf{H}(\boldsymbol{q})\ddot{\boldsymbol{q}}_c + \boldsymbol{h}(\boldsymbol{q}, \dot{\boldsymbol{q}}) + \boldsymbol{G}(\boldsymbol{q}). \tag{14}$$

Direct dynamic model of the musculoskeletal system together with the motion controller compose the biorobotic model of the vertical jump. Simulation diagram for the simulation of the vertical jump is shown in Fig. 3. Inputs into the simulation diagram are the desired trajectory of COG relative to the ankle y_{TA}^d and a signal for biarticular link activation a. Output from the simulation diagram is the vector of body's COG position $\boldsymbol{x}_T$.

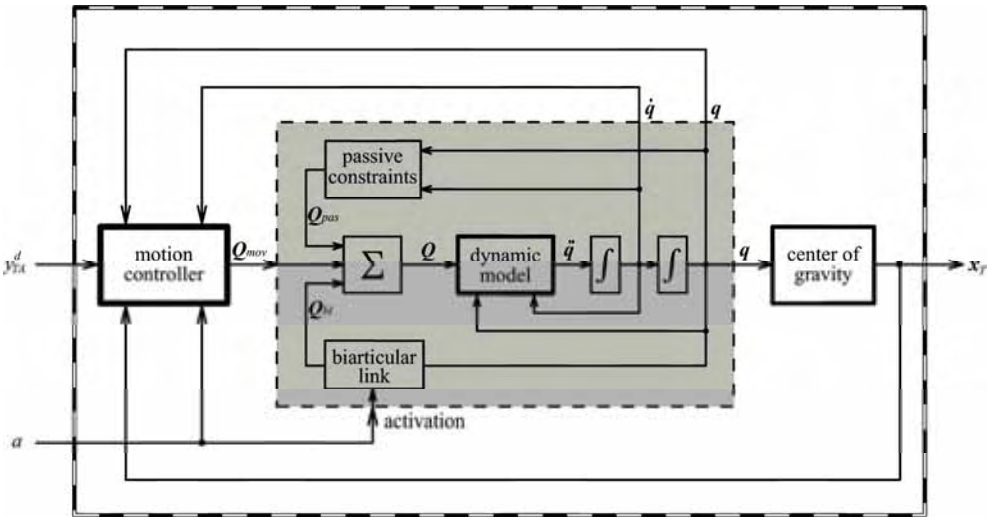

Fig. 3. Simulation diagram for the simulation of the vertical jump. Inputs into the simulation diagram are the desired trajectory of the COG relative to the ankle and a signal for biarticular link activation. Output from the simulation diagram is the vector of jumper's COG position.

3. Biomechanical Analysis of Human Vertical Jump

3.1 Subjects and Experimental Protocol

Ten trained male subjects (age 26 ± 4 years, height 180.3 ± 6.56 cm, body mass 77.1 ± 7.24 kg) participated in the study. Informed consent was obtained from all of them. The protocol of the study was approved by the National Ethics Committee of the Republic of Slovenia. The experiments comply with the current laws of the Republic of Slovenia.

After a warm-up procedure and three practice jumps, subjects subsequently performed four countermovement vertical jumps. They were instructed to keep their hands on the hips and to jump as high as possible. At the beginning of each vertical jump, subjects stood on their

toes and in the erected position. During each jump, position of anatomical landmarks over epicondylus lateralis and fifth metatarsophalangeal joint were monitored, ground reaction forces were measured and electromyogram of m. gastrocnemius was recorded. After the jumping, we determined viscoelastic properties of the triceps surae muscle tendon complex of all subjects. Details on methods and procedures are provided in the following sections.

3.2 Anthropometric Measurements

Segmental anthropometric parameters, such as masses, moments of inertia about the transverse axes, lengths and locations of the centers of gravity were estimated using regression equations (Zatsiorsky and Seluyanov 1983; Leva 1996). Position of the first metatarsophalangeal joint and the Achilles tendon insertion on the calcaneus were determined by palpation for each subject. Insertion of the m. gastrocnemius on femur was determined using the muscle data collected by Brand et al. (1982) and Delp (1990).

3.3 Kinematics and Dynamics

To determine the motion of the body's COG during the vertical jump we measured the vertical component of the ground reaction force caused by the subject during the jump. Subjects performed vertical jumps on a force platform (Kistler 9281CA) that is capable to measure ground reaction forces with the frequency of 1000 Hz. We zeroed the force platform just prior to the vertical jump when the subject was standing still in the erected position. Thus we enabled the precise determination of the subject's body mass. Body mass of the subject standing on the force platform is therefore equal to the quotient between the negative ground reaction force during the flight phase of the jump and the ground acceleration. The vertical position of the body's COG relative to the ground in time t $y_T^m(t)$ was obtained by double integrating with respect to time the vertical ground reaction force in time t $F(t)$

$$y_T^m(t) = \frac{1}{m}\int_0^t\int_0^t F(t)dtdt + y_T^m(0) \tag{15}$$

where m is the body mass of the subject and $y_T^m(0)$ is the initial height of the body's COG relative to the ground. To determine the vertical position of the body's COG relative to the ankle in time t $y_{TA}^m(t)$ we measured the motion of the ankle during the vertical jump by means of the contactless motion capture system (eMotion Smart). The vertical position of the body's COG relative to the ankle is therefore

$$y_{TA}^m(t) = y_T^m(t) - y_A^m(t) \tag{16}$$

where $y_A^m(t)$ is the vertical position of the ankle in time t.

3.4 Electromyography

The activity of the m. gastrocnemius was recorded using a pair of surface electrodes put over the medial head of the m. gastrocnemius. Analog EMG signals were amplified and filtered with a band-pass filter with cut off frequencies at 1 Hz and 200 Hz. The signals were then digitalized with 1000 Hz sampling frequency and full-wave rectified. To reduce the variability of sampled EMG signal, the signal was then smoothed with a digital low-pass Butterworth filter. Finally the EMG signal was normalized with respect to the maximum value attained during the vertical jump.

3.5 Measurements of Muscle-Tendon Viscoelastic Properties

Triceps surae muscle-tendon complex viscoelastic properties of both legs were measured for each subject using the free-vibration method described by Babič and Lenarcič (2004). The measurement device and the procedure have been designed in such a manner that as few human body segments move as possible during the measurement. Thus the measurement uncertainty due to the approximation of the properties of the human body segments was minimized. The results of the measurements are the elastic stiffness k_{GA} and viscosity b of the m. gastrocnemius and the elastic stiffness k_{AT} of the Achilles tendon.

3.6 Treatment of Data

For the purposes of analysis and optimization of the vertical jump we adjusted the biomechanical model of the musculoskeletal system with segmental anthropometric parameters, such as masses, moments of inertia about the transverse axes, lengths and locations of the centers of gravity of each subject. Parameters of the biarticular link, such as insertion of the m. gastrocnemius on femur, insertion of the Achilles tendon on calcaneus, elastic stiffness and viscosity were adjusted to match the measured parameters of each subject.

To simulate the vertical jump of the individual subject we used the measured trajectory of the body's COG as the input into the biomechanical model of the vertical jump. Biarticular link activation that is also an input into the biomechanical model of the vertical jump was determined from the EMG signal of the m. gastrocnemius. The moment of biarticular link activation was determined as the moment when the rectified, normalized and filtered EMG signal of the m. gastrocnemius increased to 95% of its maximum value. After the activation, the biarticular link remains active during the entire push-off phase of the jump.

3.7 Results

To determine the optimal timing of the biarticular link activation that results in the highest vertical jump, a series of the countermovement vertical jump simulations have been performed for each subject. Each simulation was performed with a different timing of the biarticular link activation.

All subjects activated their m. gastrocnemius slightly before the optimal moment, determined by means of simulations. In average, the difference between the optimal and measured knee angle when the m. gastrocnemius was activated was 6.4 ± 2.22˚. Because the dynamic model of the musculoskeletal system does not include the monoarticular muscle soleus, the measured heights of the jumps were higher than the jump heights determined with the simulations for 4.3 ±1.12 % in average. The primary motive for omitting the m. soleus from the modelling is that we wanted to control the motion of the body's COG relative to the ankle so that the parameters of the biarticular link could be varied and optimized for a certain measured motion of the subject's COG relative to the ankle. If the dynamic model of the musculoskeletal system would include the m. soleus, the motion of the ankle would be fully determined by the force of the m. soleus and we would not be able to control it with regard to the desired body's COG relative to the ankle. Moreover if the dynamic model of the musculoskeletal system would include the m. soleus, force produced by the m. soleus would be another input into the biomechanical model of the vertical jump and we would have to accurately measure the force produced by the m. soleus

of subjects performing the vertical jump. An additional cause for the differences between the measured heights of the jumps and the jump heights determined by means of simulations can be the simplified model of the foot that we modeled as one rigid body. The arch of the foot is linked up by elastic ligaments that can store elastic energy when deformed and later reutilize it as the mechanical work (Alexander, 1988). Ker et al. (1987) measured the deformation of the foot during running and determined the amount of the energy stored during the deformation. They showed that the elasticity of the foot significantly contribute to the efficiency of the human movement. To be able to compare the measurements and the simulation results, we corrected the simulation results by adding the contribution of the m. soleus to the height of the vertical jump. Such corrected heights of the vertical jumps at the optimal moments of m. gastrocnemius activation are insignificantly larger than the measured heights of the vertical jumps for all subjects. In average the height difference is only 1.6 ± 0.74 cm.

To determine the optimal stiffness of the Achilles tendon regarding to the height of the vertical jump, a series of the countermovement vertical jump simulations have been performed, each with a different stiffness of the Achilles tendon. Optimal timing of the biarticular link has been determined for each stiffness of the Achilles tendon as described in the previous paragraph. The measured values of the Achilles tendon stiffness for all subjects were always higher than the optimal values determined by means of simulations. By considering the elastic properties of the arch of the foot, we can assume that the optimal values of the Achilles tendon stiffness would increase and therefore the differences between the optimal and measured values would decrease.

Results of the measurements, simulations and optimizations of the human vertical jumps are presented in Fig. 4. Subjects are arranged with regard to the ratio between the optimal stiffness of the Achilles tendon determined by means of simulations and the measured stiffness of the Achilles tendon. If we want to evaluate the contribution of the viscoelastic properties to the height of the jump, ranking of the subjects with regard to the height of the jump is not appropriate because the main parameter that influences the height of the vertical jump is the power generated by muscles during the push-off phase of the jump. The elasticity of the Achilles tendon has the secondary influence on the height of the jump. Results show that for the same power generated by an individual subject during the push-off phase of the jump, the height of the vertical jump varies with the Achilles tendon stiffness. Therefore the appropriate criterion for ranking the subjects have to consider the elasticity of the Achilles tendon.

4. Simulation and Optimization of Vertical Jump

4.1 Simulation Results

Simulations of the counter movement vertical jumps were performed. At the beginning of the simulation the legs were fully straightened. A counter movement was performed until the desired minimal knee angle was reached. The flexion of the joints was such that the centre of gravity of the robot dropped with the acceleration of the gravity. Lifting of the foot from the floor would occur if faster flexions would be applied. Flexion was immediately followed by a rapid extension which provided the energy for the jump. An example trajectory of the robot center of gravity during the countermovement vertical jump is shown in Fig. 5.

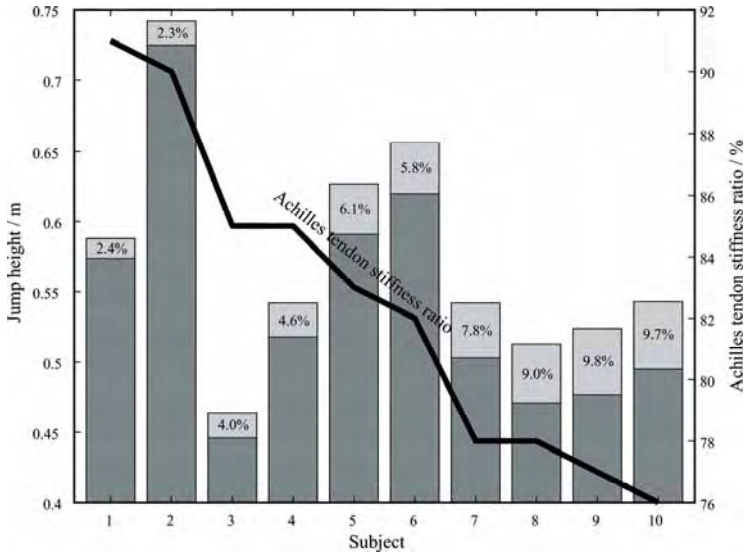

Fig. 4. Results of the measurements, simulations and optimizations of the vertical jumps. Whole bars represent the maximal heights of the vertical jumps achieved with the optimal values of the Achilles tendon stiffness and determined by means of simulations. The dark shaded parts of the bars represent the measured heights of the vertical jumps while the light shaded tops represent the differences between the maximal and measured heights of the vertical jumps. The differences are also shown as percentages relative to the measured heights. Bold line represents the ratio between the optimal stiffness of the Achilles tendon determined by means of simulations and the measured stiffness of the Achilles tendon for each subject.

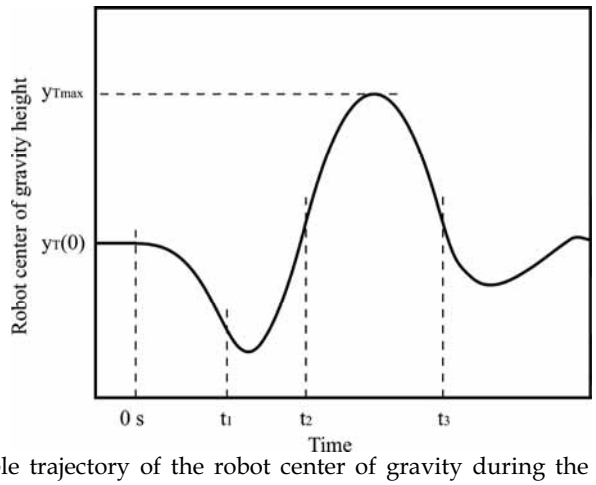

Fig. 5. An example trajectory of the robot center of gravity during the countermovement vertical jump. Time interval between 0s and t_2 represents the push-off phase of the jump while the time interval between t_2 and t_3 represents the flight phase of the jump. t_1 is the time when robot center of gravity starts to decelerate in the downward direction.

The height of the vertical jump can be calculated with the following equation

$$y_{T\,max} = y_{TA}(t_2) + y_A(t_2) - \frac{1}{2g}\left(\dot{y}_{TA}(t_2) + \dot{y}_A(t_2)\right)^2 . \quad (17)$$

As evident from (17), there are four parameters whose values in time t_2 influence the height of the vertical jump:
the height of the robot center of gravity relative to the ankle joint $y_{TA}(t_2)$,
the height of the ankle joint relative to the ground $y_A(t_2)$,
the velocity of the robot center of gravity relative to the ankle joint $\dot{y}_{TA}(t_2)$ and
the velocity of the ankle joint relative to the ground in the vertical direction $\dot{y}_A(t_2)$.
The height and the velocity of the robot center of gravity relative to the ankle joint in time t_2 depend only on the power of the actuators in the hip and knee joints while the height and the velocity of the ankle joint relative to the ground in time t_2 is the consequence of the feet motion dictated by the biarticular link. Therefore the height and the velocity of the ankle joint relative to the ground in time t_2 depend on the biomechanical parameters of the biarticular link and its activity during the push-off.

4.2 Optimization of Vertical Jump

To determine the optimum timing of the biarticular link activation that results in the highest vertical jump, a series of the countermovement vertical jump simulations have been performed, each with a different timing of the biarticular link activation. The influence of the biarticular link elasticity was eliminated by increasing the biarticular link stiffness towards the infinity. Thus we achieved a stiff biarticular link with no elastic properties. The relationship of the jump height and the biarticular link activation moment is presented in Fig. 6.

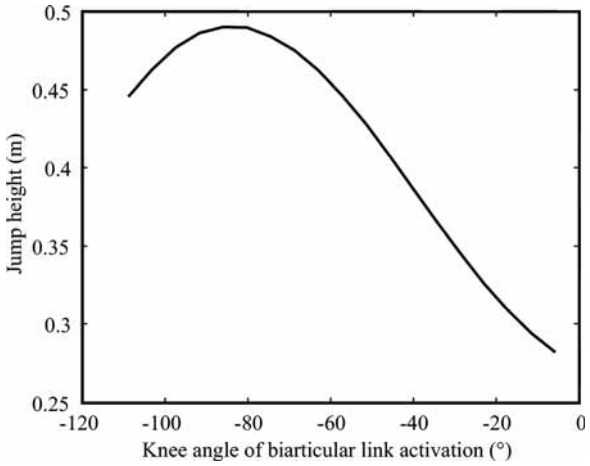

Fig. 6. Jump height as a function of the knee angle when the biarticular link is activated.

Biarticular link activation moment is presented with the knee angle when the biarticular link is activated. The highest jump has been achieved when the biarticular link was activated in the moment when the knee angle was approximately -84°. With this optimal timing, the robot jumped almost twice a high as when the biarticular link was not actuated or was

actuated when the knee was almost fully extended. If the biarticular link activates too early in the push-off phase, the robot looses its ground contact too early when its center of gravity has not reached the maximal velocity. If the biarticular link activates too late in the push-off phase, the rotational energy of the thigh and shank increases uselessly. The optimal timing represents a compromise between these two cases.

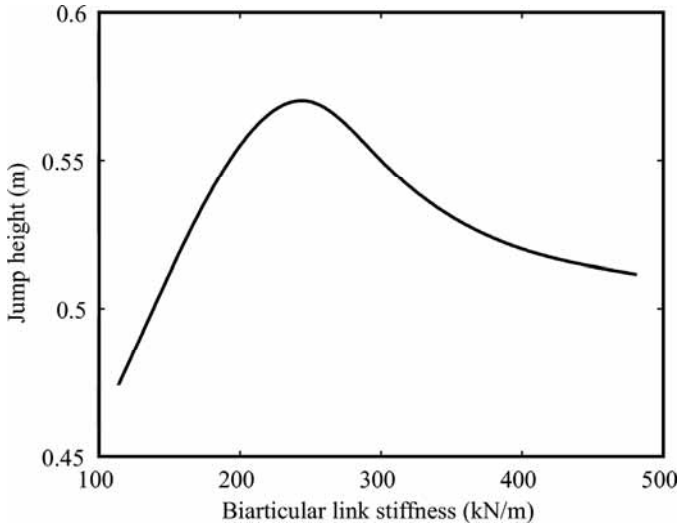

Fig. 7. Jump height as a function of the biarticular link stiffness.

To determine the optimum stiffness of the biarticular link regarding to the height of the vertical jump, a series of the countermovement vertical jump simulations have been performed, each with a different stiffness of the biarticular link. For each and every stiffness of the biarticular link the optimum timing has been determined as described in the previous paragraph. The relationship of the jump height and the biarticular link stiffness is presented in Fig. 7.

The highest jump has been achieved when the stiffness of the elastic biarticular link was approximately 245 kN/m. The highest jump was approximately 16% higher than the highest jump with the stiff biarticular link. We can thus conclude that the reutilization of the elastic energy stored during the countermovement contributes 16% to the height of the vertical jump.

4.3 Sensitivity Analysis

The purpose of the sensitivity analysis described in this section is to determine the sensitivity of the vertical jump height to the variations of the biarticular link parameters. We performed local sensitivity analysis that refers to variations of parameter around the values that ensure the maximal possible height of the vertical jump. These optimal values were determined with the optimization methods as described in the previous section. Changes of the vertical jump height that result from variations of biarticular link stiffness k, biarticular link damping b and ratio between the moment arms of the biarticular link r_C/r_B are presented in Fig. 8. Diagram in Fig. 8 also shows whether a certain parameter change results in an increase or in a decrease of the vertical jump height.

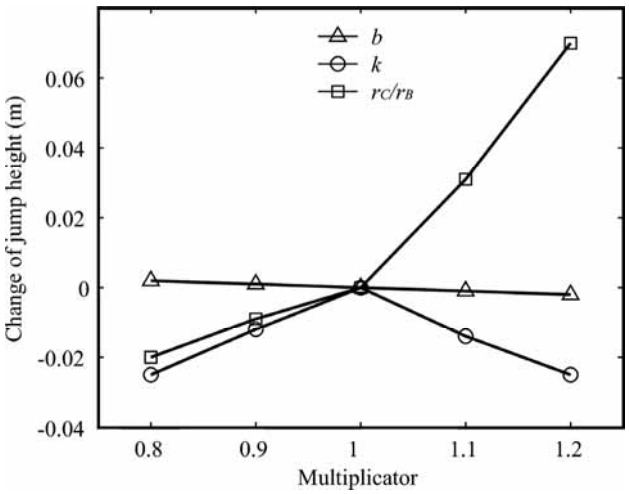

Fig. 8. Changes of vertical jump height in relation with variations of biarticular link stiffness k, biarticular link damping b and ratio between the moment arms of the biarticular link r_C/r_B. Multiplicator represents relative changes of parameter values.

As the sensitivity analysis refers to the model with optimal biarticular link stiffness, both positive and negative change of the biarticular link stiffness k cause a decrease of the jump height. An increase of the ratio between the moment arms of the biarticular link r_C/r_B causes an increase of the jump height. Higher ratio between the moment arms means higher angular speed in the ankle joint as a result or the biarticular link activation. Beside the increase of the angular speed in the ankle joint, also the force in the biarticular link increases. Variations of the biarticular link damping b only have negligible effect on the height of the vertical jump.

5. Discussion

By building an efficient biorobotic model which includes an elastic model of the biarticular muscle gastrocnemius and by simulation of the vertical jump we have demonstrated that biarticular links contribute a great deal to the performance of the vertical jump. Besides, we have shown that timing of the biarticular link activation and stiffness of the biarticular link considerably influence the height of the jump.

Methodology and results of our study offer an effective tool for the design of the humanoid robot capable of performing vertical jumps. We propose a new human inspired structure of the lower extremity mechanism that includes an elastic biarticular link and by which a humanoid robot would be able to efficiently perform fast movements such as running and jumping. However, it has to be considered that this study deals only with one biarticular link. Although the biarticular link we included in our study has the most distinctive elastic properties among all biarticular muscles of the human leg, other biarticular muscles such as the recuts femoris and the hamstrings should be included in humanoid robot design. A special challenge would be to design a humanoid lower extremity that includes all biarticular muscles of the human lower extremity and to demonstrate their joint effect on the vertical jump performance.

6. Acknowledgement

This investigation was supported by the Slovenian Ministry of Education, Science and Sport.

7. References

Alexander, R.McN. (1988). *Elastic mechanisms in animal movement,* Cambridge University Press, Cambridge

Asada, H. & Slotine, J.J.E. (1986). *Robot analysis and control*, John Wiley and sons, New York

Asmussen, E. & Bonde-Petersen, F. (1974). Storage of elastic energy in skeletal muscles in man. *Acta Physiologica Scandinavica*, 91, 385-392

Audu, M.L. & Davy, D.T. (1985). The influence of muscle model complexity in musculoskeletal motion modeling. *Journal of Biomechanical Engineering*, 107, 147-157

Babič, J. & Lenarčič, J. (2004). In vivo determination of triceps surae muscle-tendon complex viscoelastic properties. *European Journal of Applied Physiology*, 92, 477-484

Babič, J.; Karčnik, T. & Bajd, T. (2001). Stability analysis of four-point walking, *Gait & Posture*, 14, 56-60

Bobbert, M.F.; Gerritsen, K.G.M.; Litjens, M.C.A. & Soest, A.J. van (1996). Why is countermovement jump height greater than squat jump height? *Medicine & Science in Sports & Exercise*, 28, 1402-1412

Bobbert, M.F.; Hoed, E.; Schenau, G.J. van.; Sargeant, A.J. & Schreurs, A.W. (1986). A model to demonstrate the power transportating role of bi-articular muscles, *Journal of Physiology,* 387 24

Bogert, A.J. van den; Hartman, W.; Schamhardt, H.C. & Sauren, A.A. (1989). In vivo relationship between force, EMG and length change in the deep digital flexor muscle in the horse, In *Biomechanics XI-A,* G. de Groot; A.P. Hollander; P.A. Huijing; G.J. van Ingen Schenau (Eds.), pp. 68-74, Free University Press, Amsterdam

Brand, R.A.; Crowninshield, R.D.; Wittstock, C.E.; Pederson, D.R.; Clark, C.R. & Krieken, F.M. van (1982). A model of lower extremity muscular anatomy. *Journal of Biomechanics*, 104, 304-310

Cavagna, G.A. (1970). Elastic bounce of the body, *Journal of Applied Physiology*, 29, 279-282

Davy, D.T. & Audu, M.L. (1987). A dynamic optimization technique for predicting muscle forces in the swing phase of gait. *Journal of Biomechanics*, 20, 187-201

Delp, S.L. (1990). Surgery simulation: A computer graphics system to analyze and design musculoskeletal reconstructions of the lower limb, Doctoral Dissertation, Stanford University, Palo Alto

Ker, R.F.; Bennett, M.B.; Bibby, S.R.; Kester, R.C. & Alexander, R.McN. (1987). The spring in the arch of the human foot. *Nature*, 325, 147-149

Legreneur, P.; Morlon, B. & Hoecke, J. van (1997). Joined effects of pennation angle and tendon compliance on fibre length in isometric contractions: A simulation study. *Archives of Physiology and Biochemistry*, 105, 450-455

Leva, P. de (1996). Adjustments to Zatsiorsky-Seluyanov's segment inertia parameters. *Journal of Biomechanics*, 29, 1223-1230

Schenau, G.J. van. (1989). From rotation to translation: constraints of multi-joint movements and the unique action of bi-articular muscles, *Human Movement Science*, 8, 301-337

Shorten, M.R. (1985). Mechanical energy changes and elastic energy storage during treadmill running, In: *Biomechanics IXB*, D.A. Winter; R.W. Norman; R. Wells; K.C. Hayes; A. Patla (Eds.), pp. 65-70, Human Kinetics Publ, Champaign

Zatsiorsky, V. & Seluyanov, V. (1983). The mass and inertia characteristics of the main segments of the human body, In *Biomechanics VIII-B,* H. Matsui; K. Kobayashi (Eds.), pp. 1152-1159, Human Kinetics, Illinois